

Electronic Supplementary Material (ESI) for Journal of Materials Chemistry C.
This journal is © The Royal Society of Chemistry 2021

Electronic Supplementary Information (ESI)

Host-Guest Interaction-Directed Strategy for Managing Mechanochromic Luminescent Behavior by Modulating Molecular Packing and Conformation

Xie Han,^{*a,b} DongDong Sun,^a Shi Tang,^a Yong Wu,^a Luyao Wang,^a Xiongzhi Zhang,^{a,b} and Simin Liu^{*a,b}

E-mail: hanxie@wust.edu.cn; liusimin@wust.edu.cn

^a School of Chemistry and Chemical Engineering, Wuhan University of Science and Technology,
Wuhan 430081 (P.R. China)

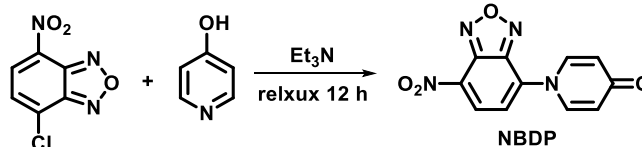
^b The State Key Laboratory of Refractories and Metallurgy, Wuhan University of Science and Technology,
Wuhan 430081 (P.R. China)

Table of Contents	Page
Table of Contents	S2
General Information	S3
Synthesis and Characterization	S3
UV/vis and Fluorescence spectra for NBDP in different solvents	S3
FTIR and absorption spectra for NBDP in the absence and presence of CB[8]	S3-4
DFT calculation for CB[8]•NBDP₂	S4-5
Absorption spectra of NBDP in the presence of CB[6], PXRD patterns	S5
Fluorescence spectra of NBDP and NBDP@CB[8] powder, table summarizing the fluorescence, PXRD patterns	S6-7
Fluorescence spectra and intermolecular interactions in NBDP-O , NBDP-G and CB[8]•NBDP₂	S7-11
NMR and EI/MS spectra of NBDP , table summarizing the main crystallographic parameters	S11-14

General Information.

CB[8] were prepared by the corresponding literature procedures.¹ Other compounds used in this study were purchased from commercial suppliers and were used without further purification. NMR spectra (¹H and ¹³C) were collected on Agilent 600 MHz DD2 spectrometers. EI-MS was obtained using Thermo scientific DSQII. UV/Vis were performed on a SHIMADZU UV-3600 instrument with 1 cm pathlength cells at 298 K. Fluorescence spectra were measured on a PerkinElmer LS-55 machine. The X-ray intensity data were measured on a Bruker APEX-II CCD system equipped with a graphite monochromator. PXRD data were collected in a Bruker D8 X-ray diffractometer using the Cu K α line ($\lambda = 1.5418 \text{ \AA}$). The quantum chemistry calculation was performed on Gaussian 16 (M06-2X/6-311G(d) basis set) software package. The interaction region plotted by independent gradient model (IGM) was analyzed by means of the Multiwfn package² and VMD software.³

Synthesis and Characterization:



Synthesis of NBDP: 4-chloro-7-nitro-2,1,3-benzoxadiazole (100 mg, 0.5 mmol), 4-Pyridinol (57 mg, 0.6 mmol) and Et₃N (0.1 mL) were dissolved in dry acetonitrile (20 mL) under a nitrogen atmosphere. The reactants were stirred and heated at reflux for 12 h. The mixture was then evaporated and purified by means of column chromatography (DCM : MeOH = 50:1, $R_f = 0.15$), as a yellow solid (62 mg, 49%). ¹H NMR (600 MHz, D₂O): δ 8.86(d, $J = 6 \text{ Hz}$, 1H), 8.48(d, $J = 12 \text{ Hz}$, 1H), 7.99 (d, $J = 6 \text{ Hz}$, 2H), 6.80 (d, $J = 6 \text{ Hz}$, 2H). ¹³C NMR (150 MHz, CDCl₃) δ (ppm): 178.94, 145.48, 143.77, 137.55, 136.51, 130.86, 120.45, 118.83. EI-MS: $m/z = 257.95 [M]^+$; calculated exact mass: 258.04.

Synthesis of NBDP@CB[8]: CB[8] solid (10 mg) was added to the aqueous solution of **NBDP** (1 mM, 1 mL) and followed by ultrasonic treatment for 5 min. The precipitate was centrifuged at 10000 rpm for 2 min and washed with DI water for 3 times, then the separated solid was dried at 60 °C.

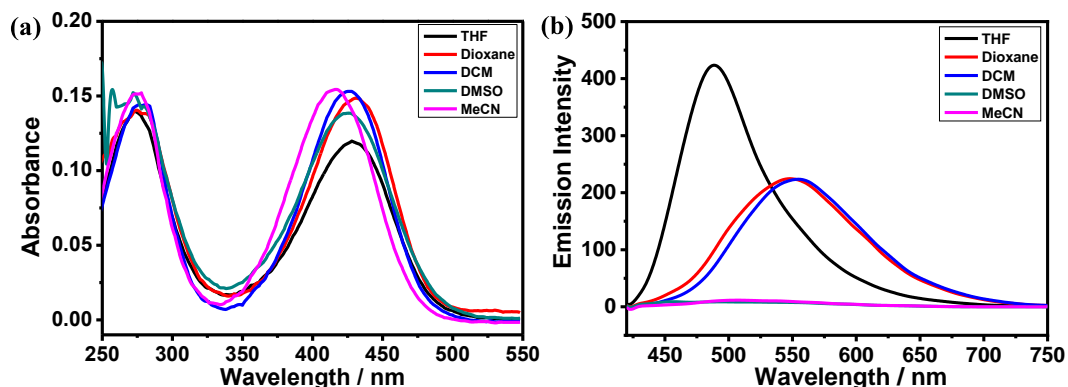


Figure S1. (a) UV/vis absorption and (b) fluorescence spectra of **NBDP** in different solvents (10 μM , $\lambda_{\text{ex}} = 420 \text{ nm}$).

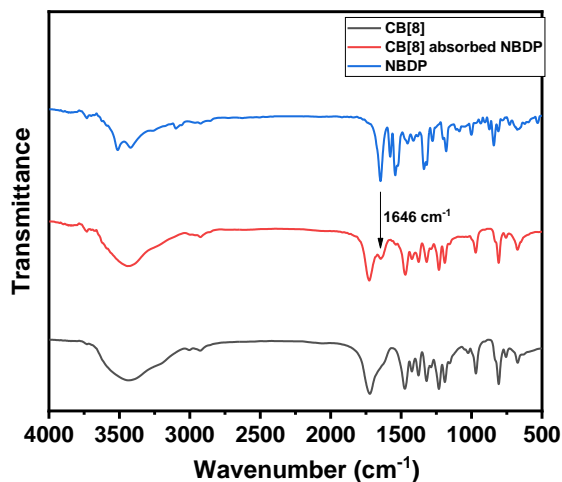


Figure S2 FTIR spectra of CB[8], **NBDP**, and CB[8] that absorbed **NBDP**.

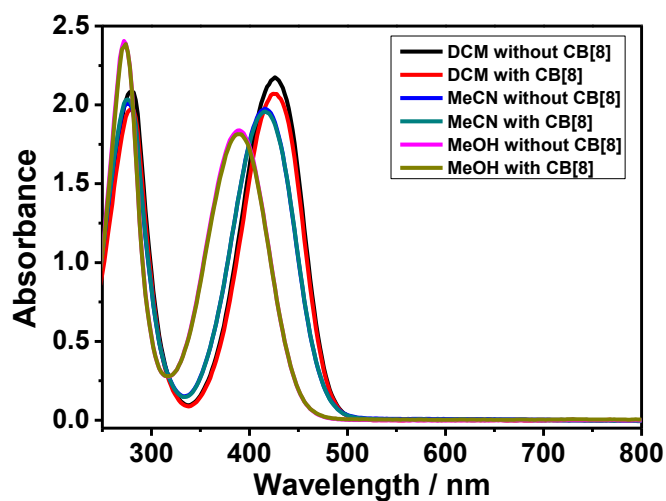


Figure S3 Absorption spectra change of **NBDP** in different solvents in the absence and presence of **CB[8]**.

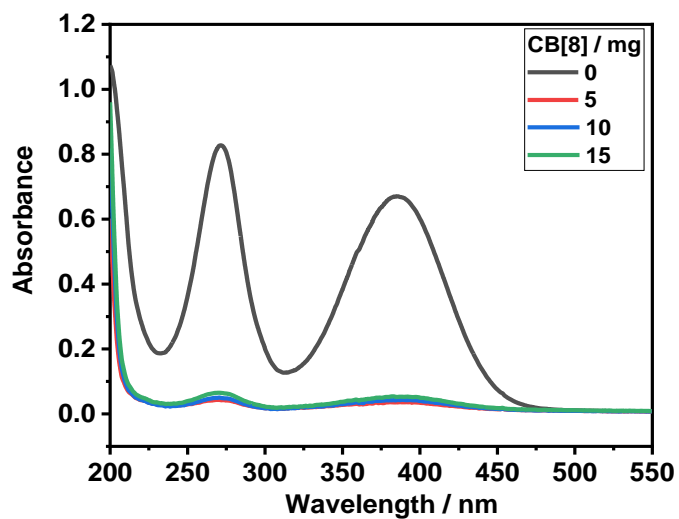


Figure S4 Absorption spectra of **NBDP** aqueous solution (1 mM, 1 mL) in the absence and presence of different equivalents of **CB[8]**.

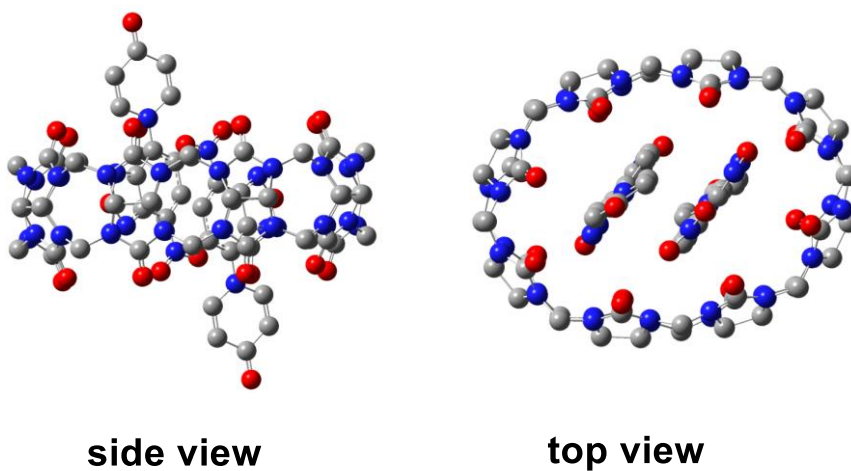


Figure S5. Molecular structures optimized by DFT calculation for **CB[8]·NBDP₂**.

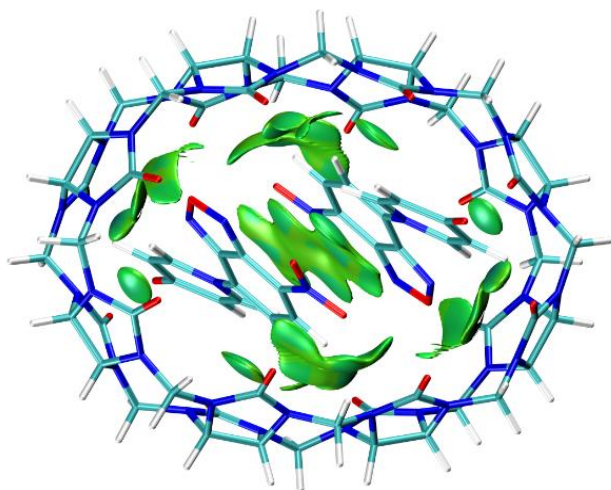


Figure S6 Independent Gradient Model (IGM) analysis of **CB[8]•NBDP₂**. Green surfaces represent the van der Waals interaction.

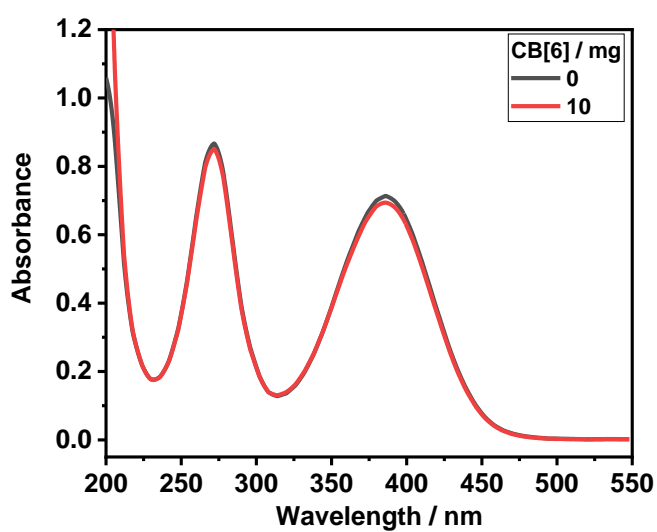


Figure S7 Absorption spectra of **NBDP** aqueous solution (1 mM, 1 mL) in the absence and presence of **CB[6]**.

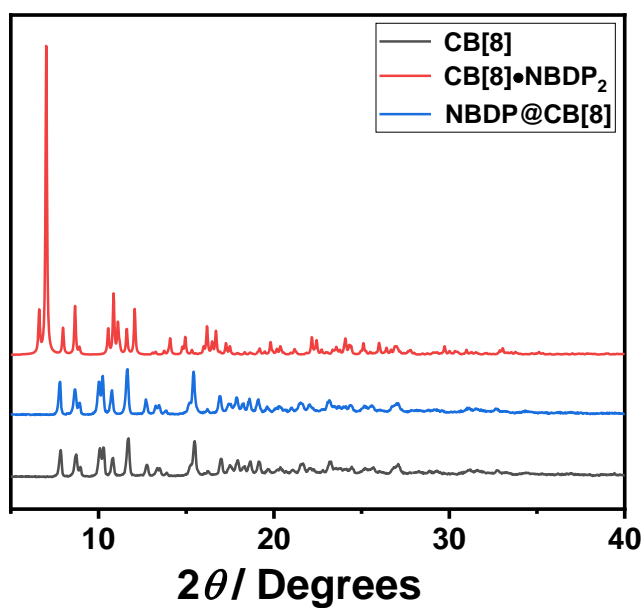


Figure S8 Powder X-ray diffraction (PXRD) patterns of **CB[8]**, **NBDP@CB[8]** powder and **CB[8]•NBDP₂** crystal (simulated from crystal structure of **CB[8]•NBDP₂**).

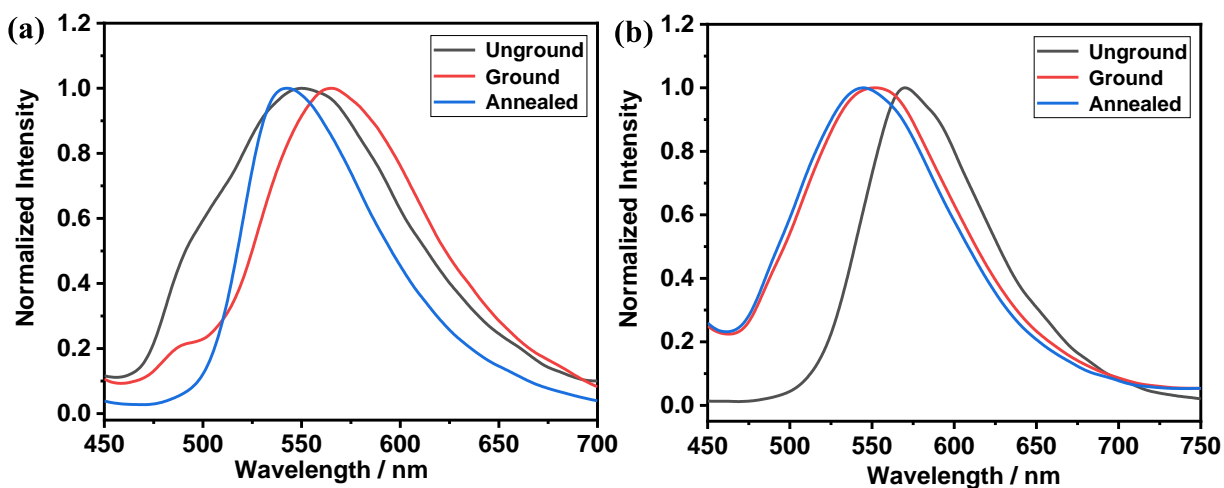


Figure S9 Normalized fluorescence spectra of (a) **NBDP** and (b) **NBDP@CB[8]** powder under different treatments.

Table S1 Fluorescence emission maxima of **NBDP** molecule in its different states.

Compound	λ_{em} (nm) (pristine) ^a	λ_{em} (nm) (ground)	Emission wavelength shift (nm)
NBDP	550	568	18
NBDP-G	534	565	31
NBDP-O	565	565	0
NBDP@CB[8]	569	548	-21 ^b
CB[8]-NBDP₂	569	579	10

^aExcited at 400 nm. ^bBlue-shift of the emission after grinding.

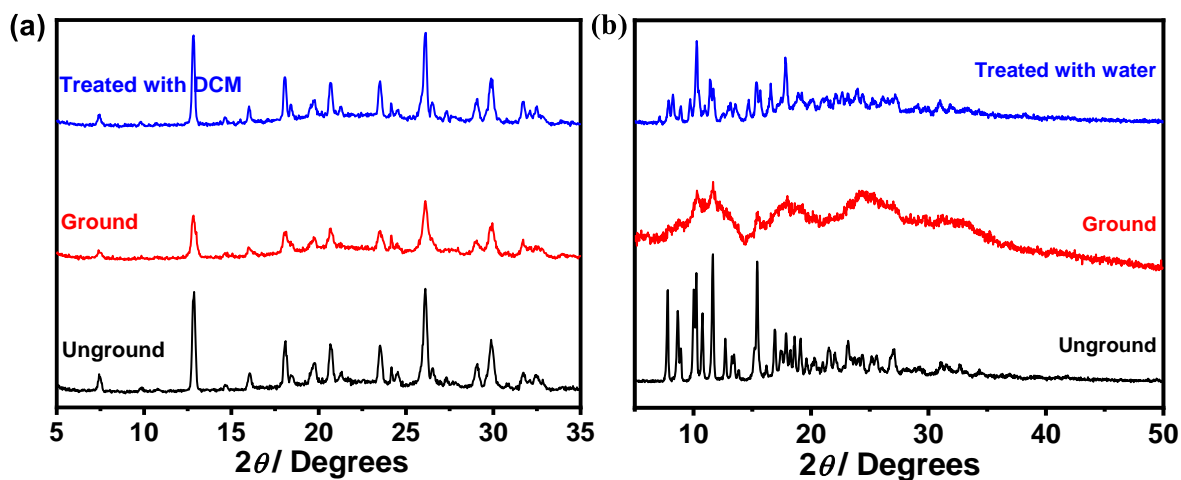


Figure S10 Powder X-ray diffraction (PXRD) patterns of (a) **NBDP** and (b) **NBDP@CB[8]** powder under different treatments.

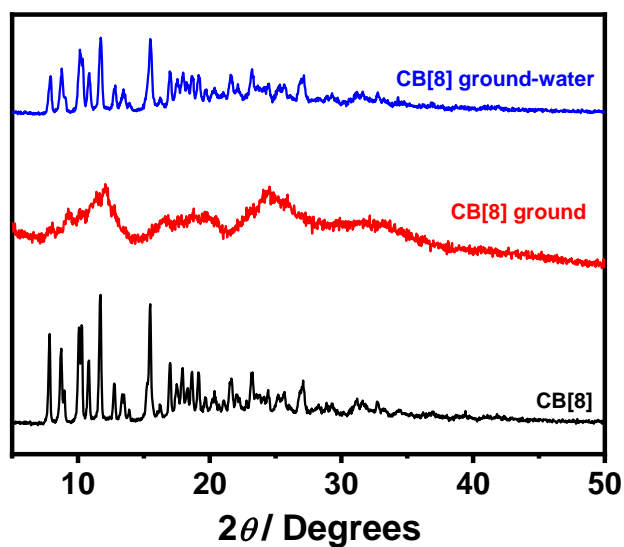


Figure S11 PXRD patterns of CB[8] powder under different treatments.

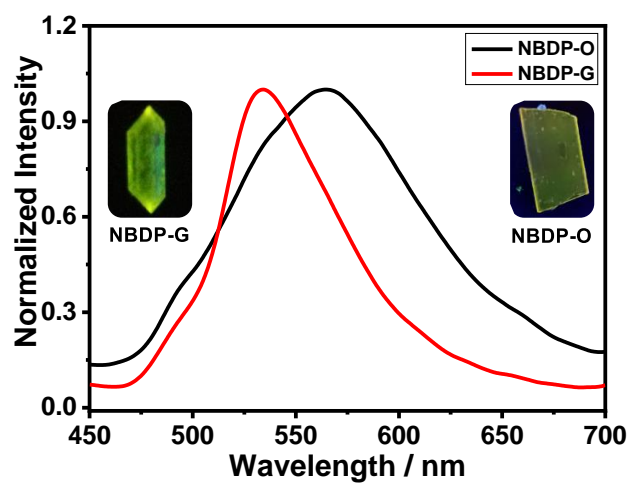


Figure S12 Normalized PL spectra of NBDP-O and NBDP-G. Insets: Fluorescence images of NBDP-O and NBDP-G under UV light (365 nm).

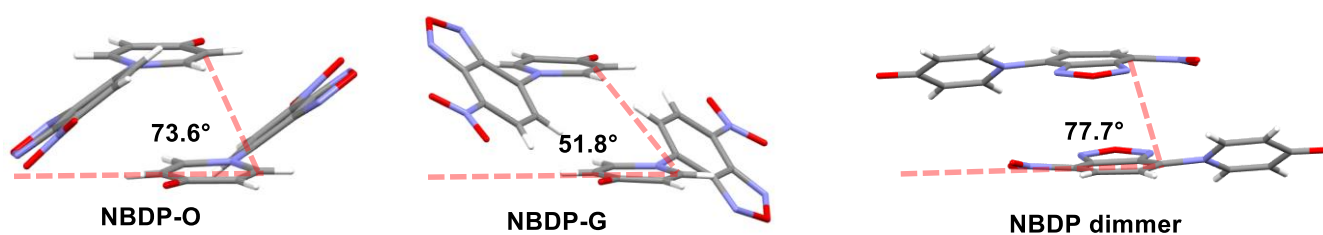


Figure S13 Slip angles of adjacent molecules in NBDP-O and NBDP-G and NBDP dimer in CB[8]·NBDP₂.

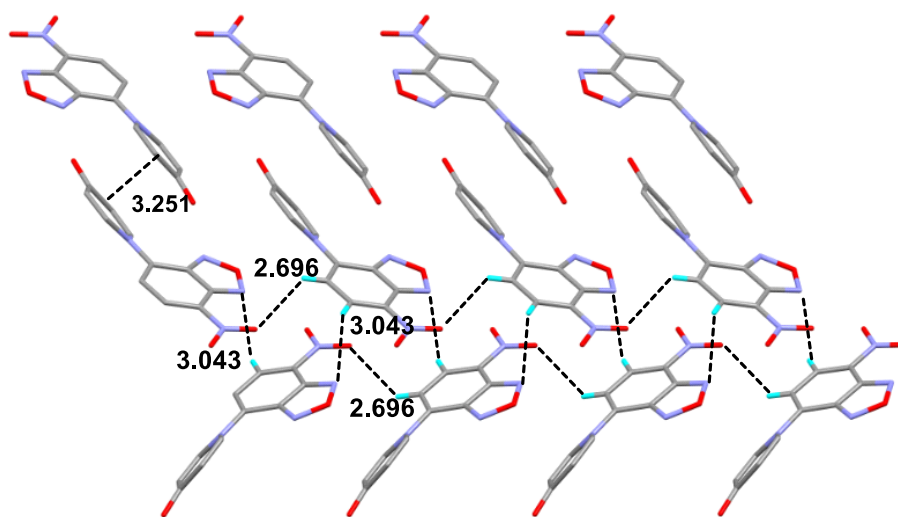


Figure S14 π - π stacking and intermolecular C-H...N, C-H...O interactions in **NBDP-O**.

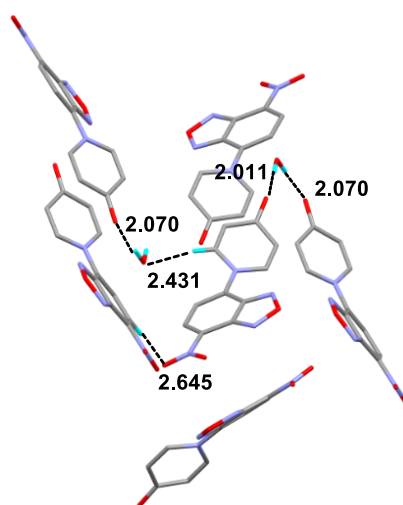


Figure S15 Intermolecular C-H...O and O-H...O interactions in **NBDP-O**.

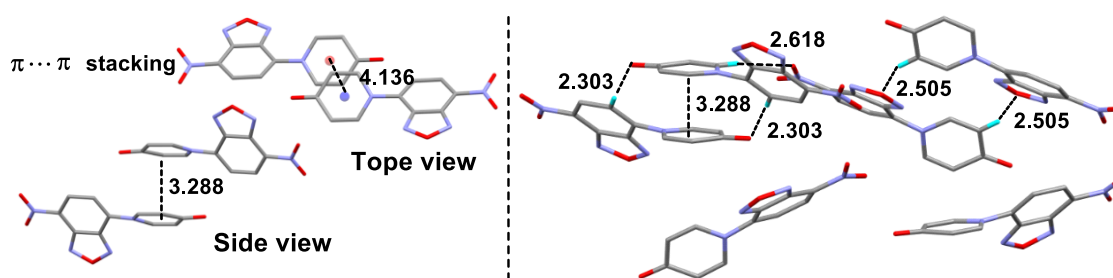


Figure S16 π - π stacking and multiple kinds of intermolecular C-H...O interactions in **NBDP-G**.

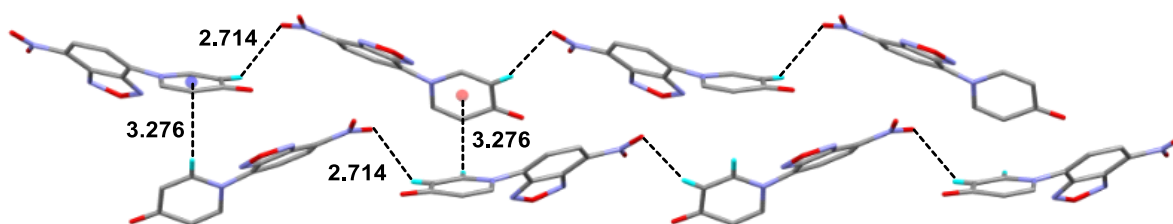


Figure S17 C-H... π and intermolecular C-H...O interactions in **NBDP-G**.

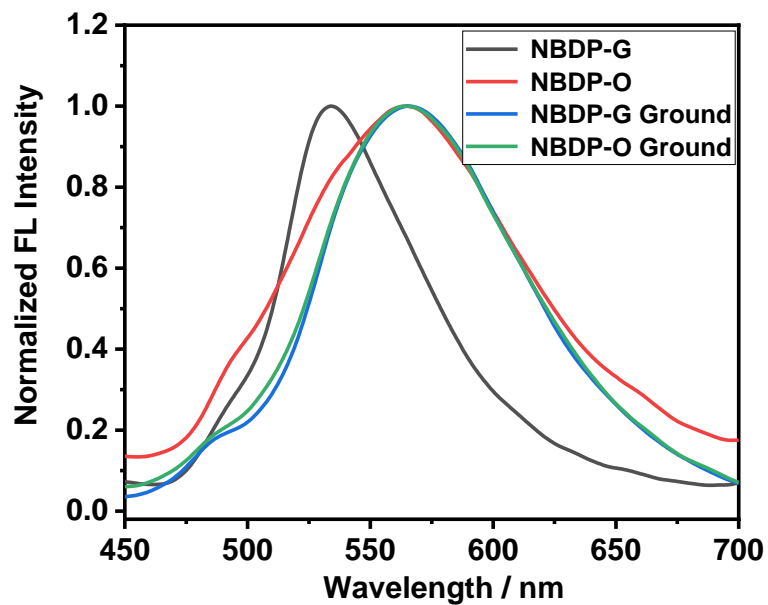


Figure S18 Normalized fluorescence spectra of NBDP-G and NBDP-O crystals before and after grinding.

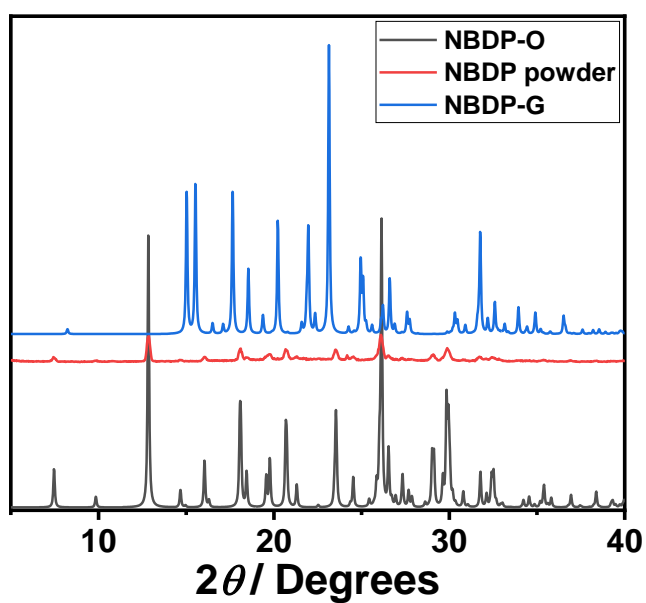


Figure S19 Powder X-ray diffraction (PXRD) patterns of NBDP powder, NBDP-O and NBDP-G crystal (simulated from crystal structure).

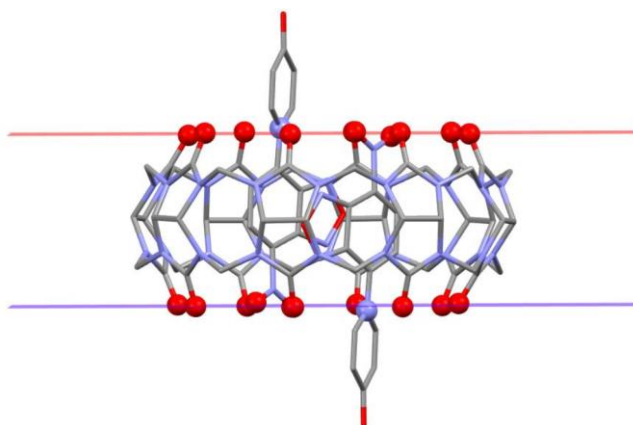


Figure S20 X-ray crystal structure of **CB[8]·NBDP₂**.

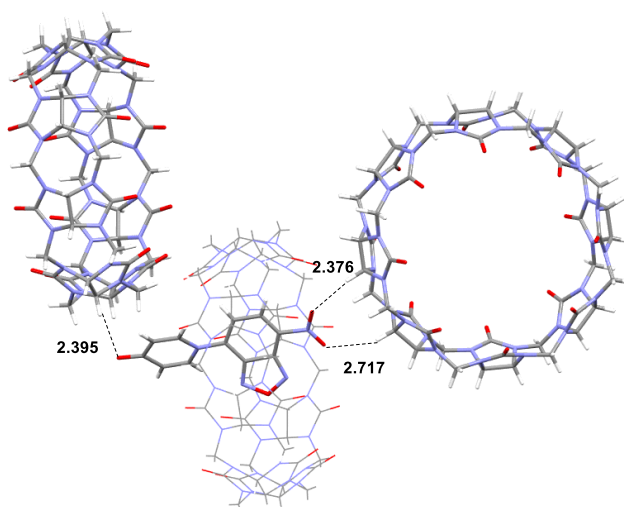


Figure S21 Intermolecular C-H...O interactions between NBDP and CB[8] host of the **CB[8]·NBDP₂** neighbors.

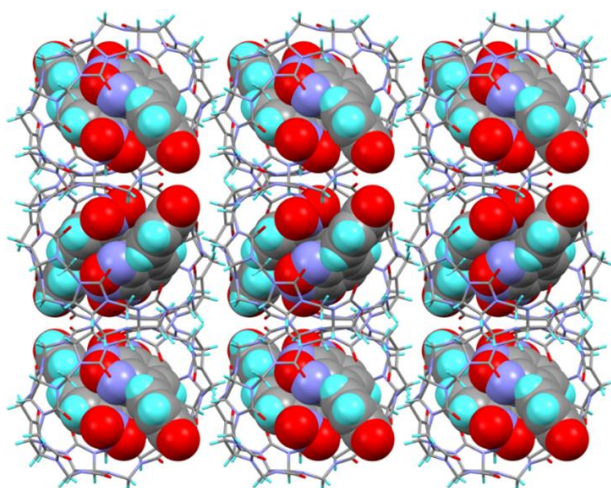


Figure S22 Molecular packing of **CB[8]·NBDP₂** complexes.

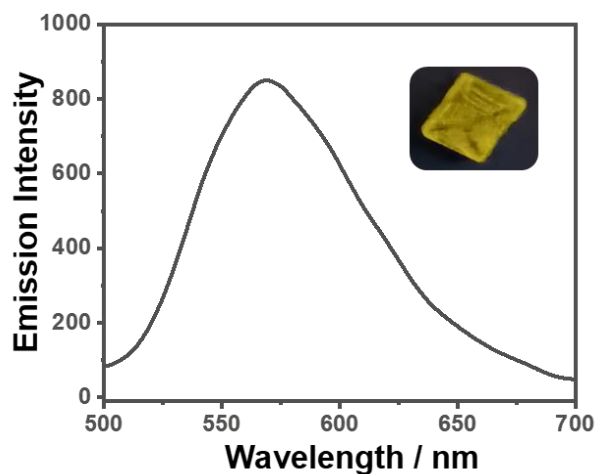


Figure S23 Fluorescence spectra of $\text{CB}[8]\cdot\text{NBDP}_2$ crystal. Insets: Fluorescence images of $\text{CB}[8]\cdot\text{NBDP}_2$ crystal under UV light (365 nm).

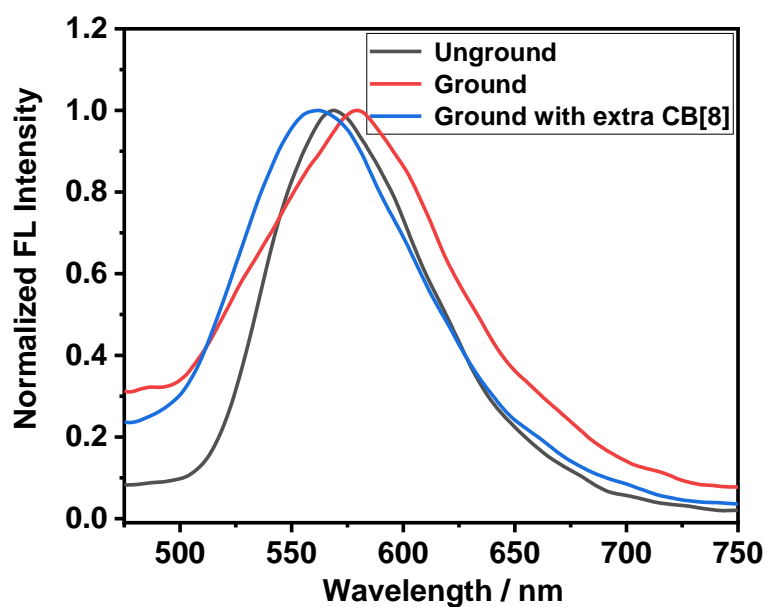


Figure S24 Normalized fluorescence spectra of $\text{CB}[8]\cdot\text{NBDP}_2$ crystal under different treatments.

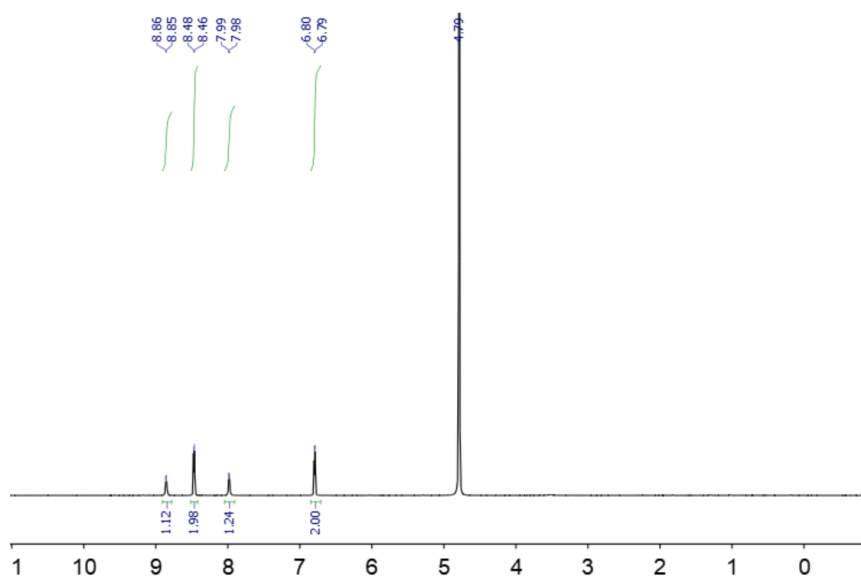


Figure S25 ^1H NMR (600 MHz, D_2O) of NBDP.

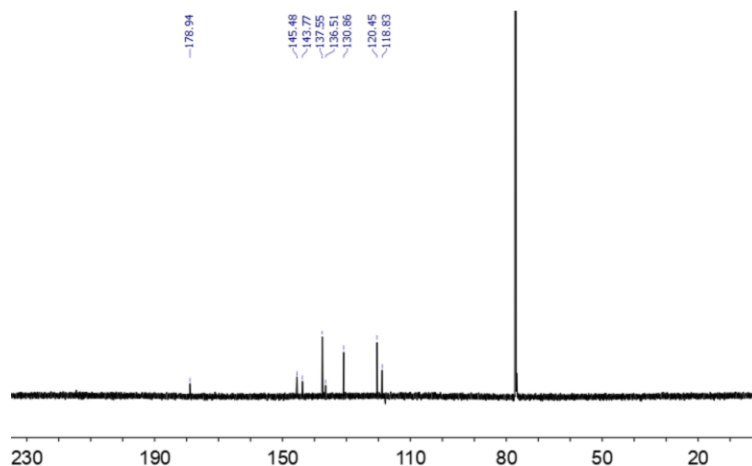


Figure S26 ^{13}C NMR (150 MHz, CDCl_3) spectra of NBD-O.

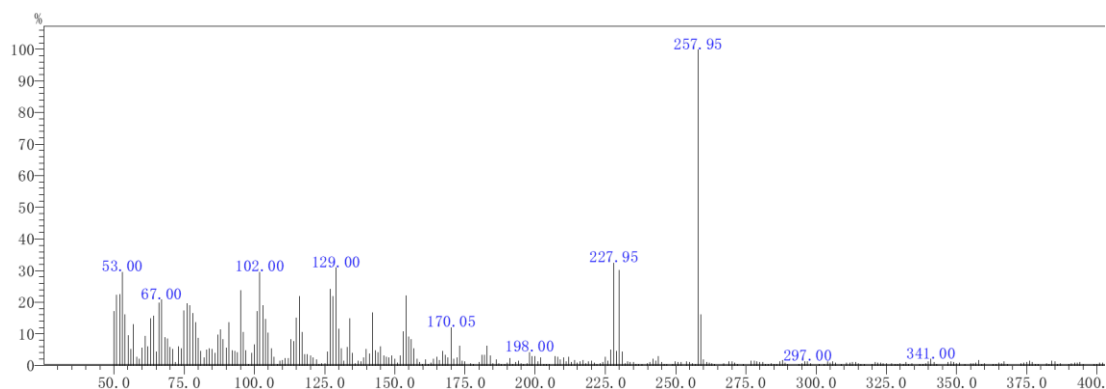


Figure S27 EI/MS spectra of NBD-O.

Table S2 The main crystallographic parameters of NBD-O

Identification code	NBD-O
Empirical formula	$\text{C}_{11}\text{H}_8\text{N}_4\text{O}_5$
Formula weight	276.21
Temperature/K	296.15
Crystal system	orthorhombic
Space group	Pbca
a/Å	13.774(2)
b/Å	6.9990(11)
c/Å	23.662(4)
$\alpha/^\circ$	90
$\beta/^\circ$	90
$\gamma/^\circ$	90
Volume/Å ³	2281.1(6)
Z	8
$\rho_{\text{calc}}/\text{cm}^3$	1.609
μ/mm^{-1}	0.131
F(000)	1136.0
Crystal size/mm ³	0.3 × 0.2 × 0.1
Radiation	MoK α ($\lambda = 0.71073$)
2 Θ range for data collection/ $^\circ$	4.538 to 60.87
Index ranges	-13 ≤ h ≤ 19, -9 ≤ k ≤ 9, -33 ≤ l ≤ 33
Reflections collected	16732
Independent reflections	3339 [$R_{\text{int}} = 0.0265$, $R_{\text{sigma}} = 0.0206$]
Data/restraints/parameters	3339/0/184
Goodness-of-fit on F^2	1.041
Final R indexes [$I > 2\sigma(I)$]	$R_1 = 0.0424$, $wR_2 = 0.1368$

Final R indexes [all data]	$R_1 = 0.0639$, $wR_2 = 0.1533$
Largest diff. peak/hole / e \AA^{-3}	0.25/-0.18

Table S3 The main crystallographic parameters of **NBD-G**

Identification code	NBD-G
Empirical formula	$C_{11}H_6N_4O_4$
Formula weight	258.20
Temperature/K	296.15
Crystal system	orthorhombic
Space group	Pbca
a/ \AA	8.7743(5)
b/ \AA	11.8277(7)
c/ \AA	21.4669(13)
$\alpha/^\circ$	90
$\beta/^\circ$	90
$\gamma/^\circ$	90
Volume/ \AA^3	2227.8(2)
Z	8
$\rho_{\text{calc}}/\text{g/cm}^3$	1.540
μ/mm^{-1}	0.122
F(000)	1056.0
Crystal size/ mm^3	0.1 × 0.05 × 0.05
Radiation	MoK α ($\lambda = 0.71073$)
2 Θ range for data collection/ $^\circ$	3.794 to 55.194
Index ranges	-6 ≤ h ≤ 11, -15 ≤ k ≤ 13, -19 ≤ l ≤ 26
Reflections collected	9910
Independent reflections	2319 [$R_{\text{int}} = 0.0245$, $R_{\text{sigma}} = 0.0281$]
Data/restraints/parameters	2319/0/173
Goodness-of-fit on F^2	1.004
Final R indexes [$l > 2\sigma(l)$]	$R_1 = 0.0406$, $wR_2 = 0.0937$
Final R indexes [all data]	$R_1 = 0.0831$, $wR_2 = 0.1123$
Largest diff. peak/hole / e \AA^{-3}	0.14/-0.15

Table S4 The main crystallographic parameters of **CB[8]·NBDP₂**

compound	CB[8]·NBDP₂
Empirical formula	$C_{70}H_{60}N_{40}O_{24}$
Formula weight	1845.58
Temperature/K	296.15
Crystal system	monoclinic
Space group	P2 ₁ /c
a/ \AA	13.794(3)
b/ \AA	19.827(5)
c/ \AA	16.822(4)
$\alpha/^\circ$	90
$\beta/^\circ$	104.599(7)
$\gamma/^\circ$	90
Volume/ \AA^3	4452.1(17)
Z	2
$\rho_{\text{calc}}/\text{g/cm}^3$	1.377
μ/mm^{-1}	0.108
F(000)	1904.0
Crystal size/ mm^3	0.1 × 0.1 × 0.1
Radiation	MoK α ($\lambda = 0.71073$)
2 Θ range for data collection/ $^\circ$	4.108 to 50
Index ranges	-16 ≤ h ≤ 15, -23 ≤ k ≤ 23, -19 ≤ l ≤ 20

Reflections collected	27742
Independent reflections	7783 [$R_{\text{int}} = 0.0938$, $R_{\text{sigma}} = 0.0955$]
Data/restraints/parameters	7783/0/604
Goodness-of-fit on F^2	1.114
Final R indexes [$I \geq 2\sigma(I)$]	$R_1 = 0.1090$, $wR_2 = 0.2652$
Final R indexes [all data]	$R_1 = 0.1385$, $wR_2 = 0.2868$
Largest diff. peak/hole / $e \text{ \AA}^{-3}$	0.57/-0.48

References

- [1] A. Day, A.P. Arnold, R.J. Blanch and B. Snushall, *J. Org. Chem.* 2001, **66**, 8094–8100
- [2] T. Lu and F. Chen, *J. Comput. Chem.* 2012, **33**, 580-592
- [3] W. Humphrey, A. Dalke and K. Schulten, *J. Mol. Graphics Modell.* 1996, **14**, 33-38